

2021

## Design of Capacitive Sensors for Measuring Void Fraction in Headers of Microchannel Heat Exchangers

Hongliang Qian

*University of Illinois at Urbana and Champaign*, [hqian7@illinois.edu](mailto:hqian7@illinois.edu)

Pega Hrnjak

*University of Illinois at Urbana and Champaign*

Follow this and additional works at: <https://docs.lib.purdue.edu/iracc>

---

Qian, Hongliang and Hrnjak, Pega, "Design of Capacitive Sensors for Measuring Void Fraction in Headers of Microchannel Heat Exchangers" (2021). *International Refrigeration and Air Conditioning Conference*. Paper 2150.  
<https://docs.lib.purdue.edu/iracc/2150>

This document has been made available through Purdue e-Pubs, a service of the Purdue University Libraries. Please contact [epubs@purdue.edu](mailto:epubs@purdue.edu) for additional information. Complete proceedings may be acquired in print and on CD-ROM directly from the Ray W. Herrick Laboratories at <https://engineering.purdue.edu/Herrick/Events/orderlit.html>

## Design of Capacitive Sensors for Measuring Void Fraction in Headers of Microchannel Heat Exchangers

Hongliang QIAN<sup>1</sup>, Pega HRNJAK<sup>1, 2\*</sup>

<sup>1</sup>Air Conditioning and Refrigeration Center, the University of Illinois at Urbana-Champaign, 1206 West Green Street, Urbana, IL 61801, USA

<sup>2</sup>Creative Thermal Solutions, 2209 Willow Rd., Urbana, IL, USA

\* Corresponding Author: pega@illinois.edu +1-217-390-5278

### ABSTRACT

This paper presents the design and building of capacitive sensors for measuring void fraction in headers of microchannel heat exchangers with R134a. The capacitive sensors utilize different electrical properties (dielectric constant) between the liquid and vapor phases to measure the void fraction of two-phase flow. The test section (a header) is made of 3D printed partitions with a total length of 185.8 mm and an inner diameter of 15.8 mm (D). It has eleven microchannel-tube protrusions with a depth of half inner diameter. All microchannel tubes are capable of being connected to real aluminum tube-like real heat exchangers in the future study. Eleven capacitive sensors locate between protrusions. Each sensor has two concave-plate electrodes with the axial length of the half inner diameter (D/2). With these eleven sensors, void fractions along the header can be measured spontaneously. Preliminary validation of the sensors is also presented in this paper.

### 1. INTRODUCTION

Microchannel heat exchangers (MCHEs) are widely used in the AC&R system. They have the advantages of compactness, the potential for charge reduction, and enhancement of heat transfer performance. Good prediction models for the charge in microchannel tubes were proposed in the previous studies. However, the prediction models of charge in headers are still missing. The former analysis also indicates around 70% of the charge in a typical MCHE is in the headers (Hrnjak & Litch, 2008). Hence, the refrigerant inventory in the headers is a very important part of modeling the charge of the entire MCHE. Void fractions and flow regimes along the headers are two of the essential parameters closely related to the charge. Due to the complex header geometries and refrigerant flow patterns within the headers, no open literature reported a systematic way to measure refrigerant void fractions in the headers to our best knowledge.

The capacitive method is a nonintrusive way to measure void fraction and detect flow regimes in two-phase flow at a lower cost. This method usually does not involve safety issues and is easy to implement. It utilizes different electrical properties (permittivity or dielectric constant) between the liquid and vapor phases. Many researchers (Abouelwafa & Kendall, 1980; Canière *et al.*, 2007; Canière *et al.*, 2008; De Kerpel, 2015; Jaworek & Krupa, 2004, 2010; Olivier *et al.*, 2015; Qian & Hrnjak, 2020, 2021) designed capacitance sensors to measure void fractions or detect flow regime for two-phase flows for tubes. Various sensor designs (electrodes configurations, Figure 1) and electrical measuring circuits (transmitter/transducer) were proposed. In this paper, the previous work on the sensor for smooth tubes (Qian & Hrnjak, 2020) is summarized first. Then the new capacitive sensor for headers is presented.

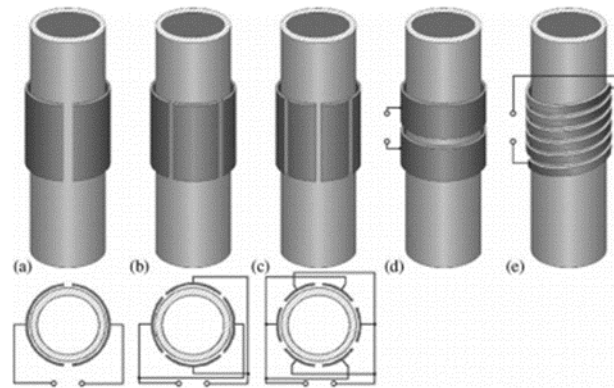


**Figure 1:** Some typical electrode configurations (Jaworek & Krupa, 2004). (a) Two concave plates. (b) Four concave plates. (c) Six concave plates. (d) Rings. (e) Double helix

## 2. CAPACITIVE SENSORS FOR SMOOTH TUBES

The two-concave-plate configuration (Figure 1a) is selected for the sensors for both tubes and headers. In comparison to other configurations, it is relatively easier to be built, especially for sensors installed on smaller tubes or complicated geometries. It has higher sensitivity compared to the double-helix configuration (Abouelwafa & Kendall, 1980). Furthermore, if the axial length of the sensors is reduced, sensors with this configuration will have the possibility to measure the cross-sectional void fraction. The capacitive sensor for smooth tubes is based on the work from Canière et al. (2007). Some modifications and further developments are made to make the sensor suitable for more configurations other than only for horizontal tubes (Qian & Hrnjak, 2020). Figure 2 shows the cross-sectional and side view of the capacitive sensor for circular tubes. The two-phase refrigerant flows in a thin tube (diameter of  $D$ ) made by a dielectric layer. Sensors (two concave electrodes, each with a central angle of  $\beta$ ) are outside the dielectric layer, connecting to copper wires. The outermost layer is a grounded metal shield.

Canière (2010) selected the axial length of electrodes ( $L$ ) equal to one inner diameter ( $D$ ) and claimed it could be further reduced if the transducer could be improved. Many studies in the literature used two-concave-plate configuration sensors with an axial length of more than one diameter. In the previous study (Qian & Hrnjak, 2020, 2021), three sensors with an axial length of one inner diameter ( $D$ ),  $2D/3$ , and  $D/2$  are tested. The results show that a shorter sensor ( $D/2$ ) can measure void fractions and characterize flow regimes as the larger ones ( $D$ ). Some key parameters of the sensor for smooth tubes: dielectric layer thickness  $t$ , electrode angle  $\beta$ , shield diameter  $R$ , and electrode axial length  $L$  are listed in Table 1.

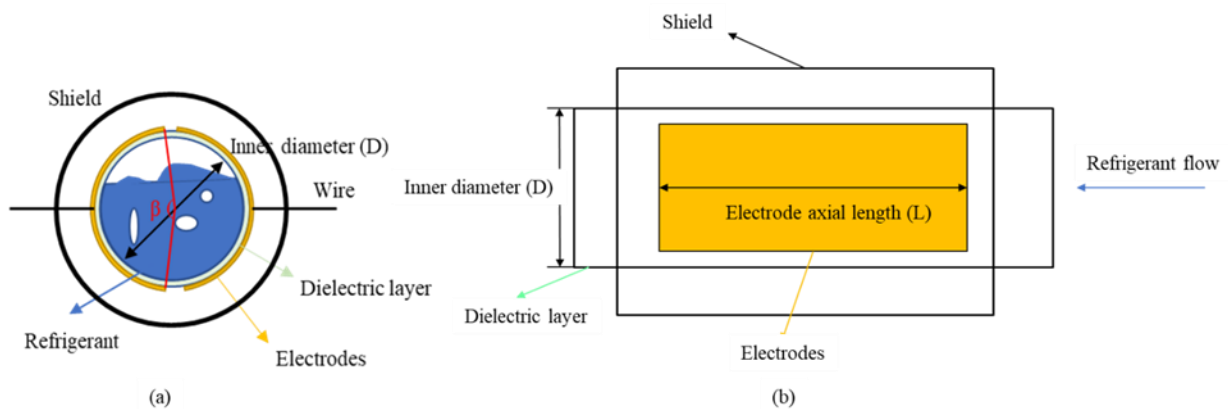


**Figure 2:** Cross-sectional (a) and side view (b) of the capacitive sensor

**Table 1:** Dimensions of the sensor for smooth tubes

Key parameter	Inner tube diameter, D	Electrode axial length, L	Electrode angle, $\beta$	Dielectric layer thickness, t	Shield inner diameter, R
Dimension	7 mm	D, 2D/3, D/2	160°	0.05 mm	42.8 mm

### 3. CAPACITIVE SENSORS FOR HEADERS

The cross-sectional void fraction is changing along the headers of microchannel heat exchangers. It is necessary to measure the local void fraction between two tubes to determine refrigerant variation. In other words, many individual capacitive sensors that can provide independent signals and measure the local void fraction need to locate between two tube protrusions. Hence, the tested header is designed to be divided into small partitions. Each partition has a microchannel tube and a sensor. After all parts are built, they are assembled to be a single header.

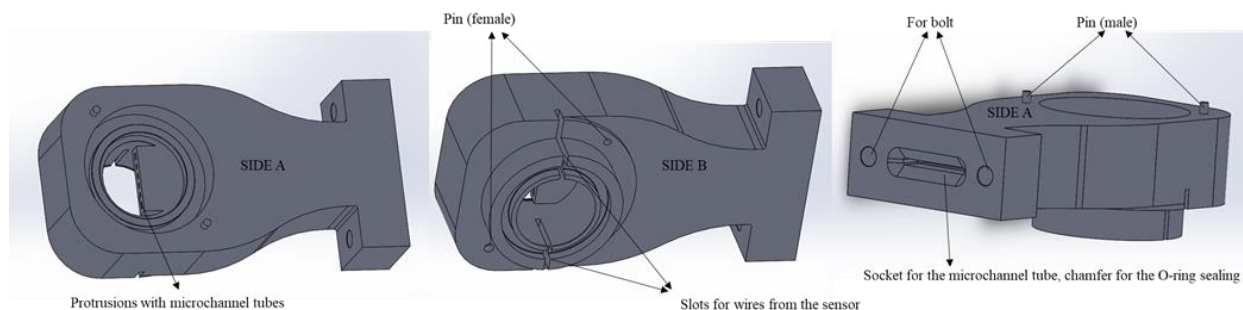
Besides the header with sensors, pressure drop, and visualization results along the header are necessary to study void fraction. However, with the sensor installed within the header, it is difficult to obtain pressure drop and visualization results simultaneously. Hence, another 3D-printed and fully transparent test section with pressure measurement ports is also built. These two tested parts have the same inner geometry and will be installed at the same height in the facility with the same inlet tubes. By controlling valves, refrigerant can pass through either loop. The void fractions and flow regimes are assumed to be the same for the same tested conditions. Detailed facility schematics and calibration procedures are discussed in the next paper.

#### 3.1 Design and building of capacitive sensor

Eleven individual partitions without sensors are 3D printed. The 3D view and schematic drawing of the partition are shown in Figures 3 and 4. The inner diameter is 16.2 mm, which is slightly larger than the desired header diameter, 15.8 mm. The extra space is for sensors installed inside. Two slots are kept open for the wires to be connected to the sensor. On sides A and B, two pins are built to ensure the header part is concentric when assembled. The tube protrusion, with a thickness of 3 mm and a width of 13.6 mm, has six open microchannels. It protrudes halfway of the inner diameter. At the other end of the 3D printed microchannel tube, there is a socket for the aluminum microchannel tube connection and a chamfer for the sealing with an O-ring. Two holes are made for the bolt and nut connection like a flange.

Figures 5 and 6 show the 3D view and schematic of the capacitive sensor. The dielectric layer and electrodes are made by the laminate circuit material Ultralam® 3850. The capacitive sensor design is based on the same principle as the former sensor for smooth tubes mentioned in the last section. The sensor has two concave-plate electrodes, which are made from copper. The precise shape and location of electrodes on a dielectric layer are achieved by the etching technique. One copper wire is soldered onto each electrode to transfer signals from the sensor to the transmitter. The electrodes are built on a thin dielectric layer (thickness of 0.05 mm). Refrigerant will flow within the dielectric layer. The inner diameter (D) is 15.8 mm. The sensor axial length is D/2, 7.9 mm. The electrode angle,  $\beta$ , is 160°.

The assembly of the individual partitions with the capacitive sensor and aluminum microchannel tube is shown in Figure 7. In this way, one sensor is utilized to measure the local void fraction and characterize flow regimes between protrusions.

**Figure 3:** 3D view of the partition without the sensor

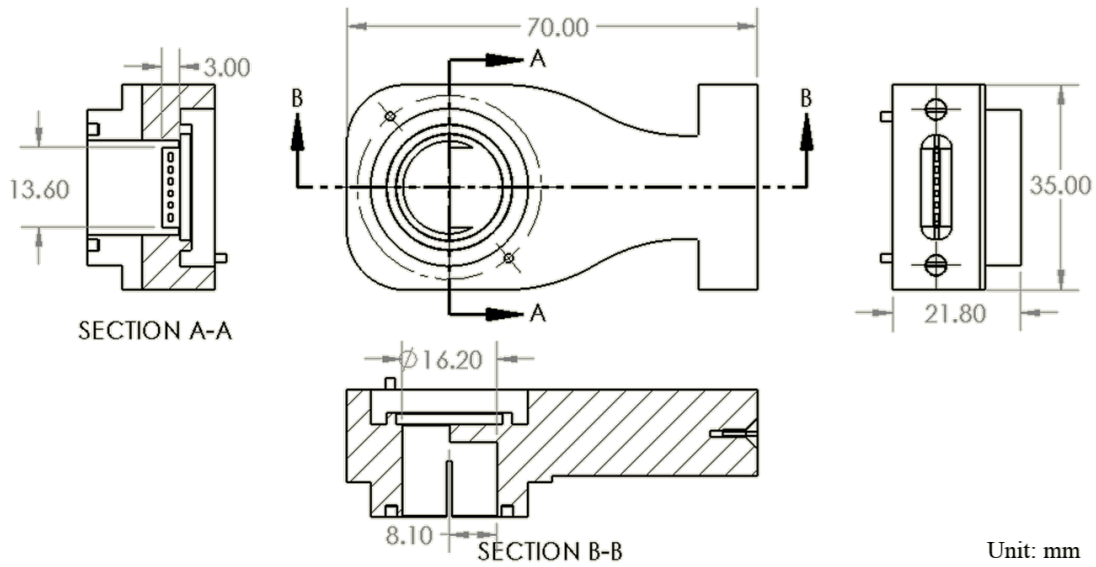


**Figure 4:** Schematic and dimensions of the partition without the sensor

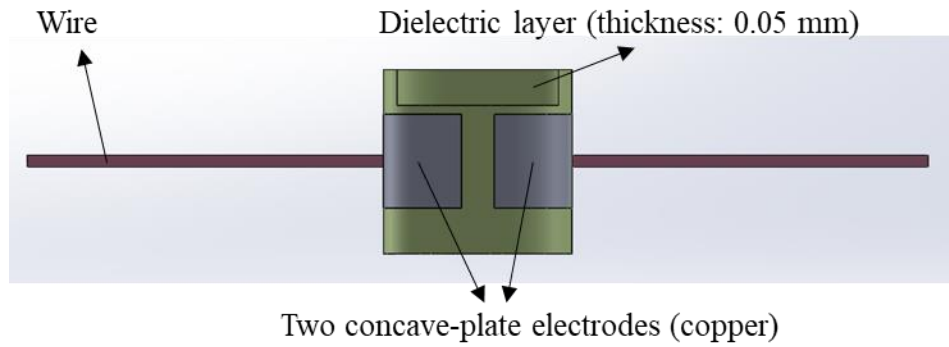


**Figure 5:** 3D view of the individual capacitive sensor

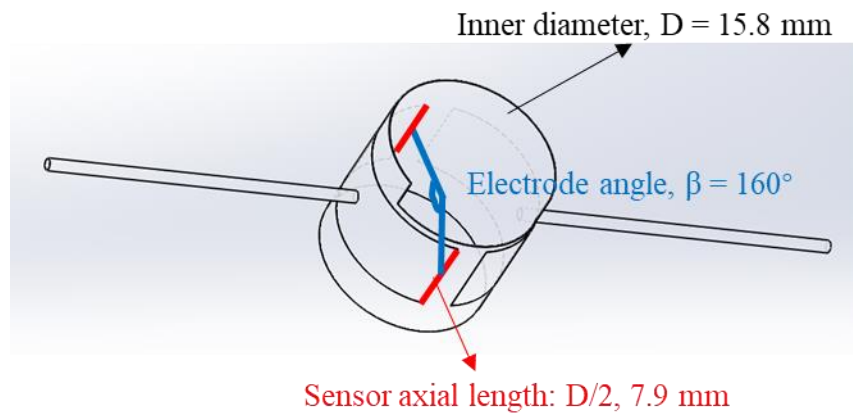


**Figure 6:** Schematic and dimensions of the individual sensor

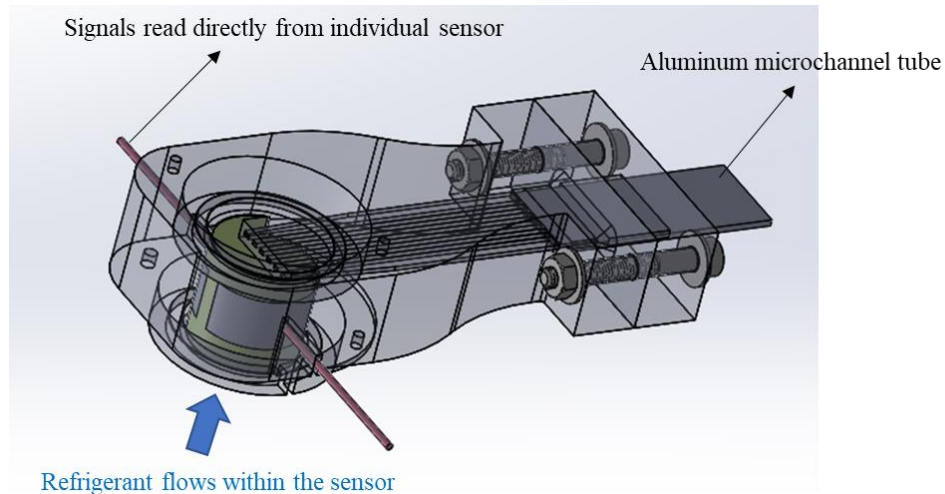


**Figure 7:** Individual partition with the sensor and aluminum microchannel tube installed

After all 11 individual partitions are made, they are assembled into a header (Figure 8). The pitch between two protrusions or two sensors is 15.8 mm, which is the same as the inner tube diameter ( $D$ ). The microchannel tubes are blocked for calibration purposes. The calibration procedure of the sensors is reported in the next paper. A piece of aluminum tube that is connected to the ground is put outside the header as a shield to reduce the environmental influence. The gap between the header and the aluminum tube is filled with resin to make this structure more robust. A metal frame is utilized to connect the tested header to the facility. Two valves are located right outside the metal frame as two Quick-closing valves (QCV) to measure average void fractions inside the header. A 1/8" ball valve with minimal connecting tube is installed at the bottom of the header to recycle refrigerant in the QCV method. The detailed average void fraction measurement procedure with QCV is reported in the former study (Qian & Hrnjak, 2019). The final assembled tested header with sensors and quick-closing valves is shown in Figure 9.



**Figure 8:** Header assembled from individual partitions

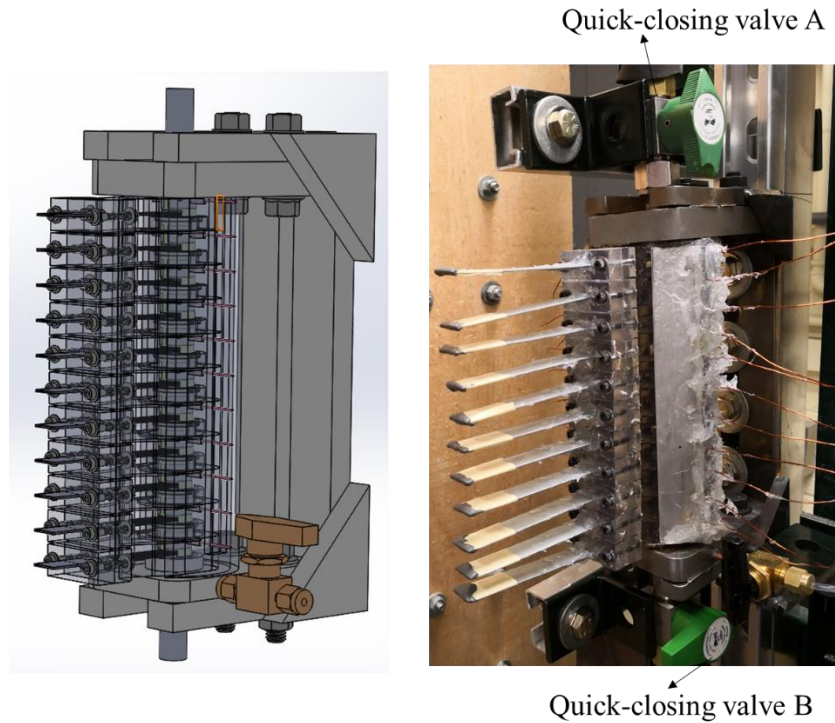


**Figure 9:** Tested header part with sensors and two quick-closing valves

### 3.2 Visualization and pressure drop measurement part

As mentioned above, pressure drop measurements and flow regime visualizations are essential to the void fraction measurements in the headers. However, due to the intransparency and complexity of the sensor, it is more reasonable to obtain pressure drop and flow regimes in a separate test part (Figure 10). It is a fully transparent 3D part with the same inner geometry as the sensor part. The microchannel tubes are also blocked for now. It can be easily opened and connected to real aluminum tubes in the future study.

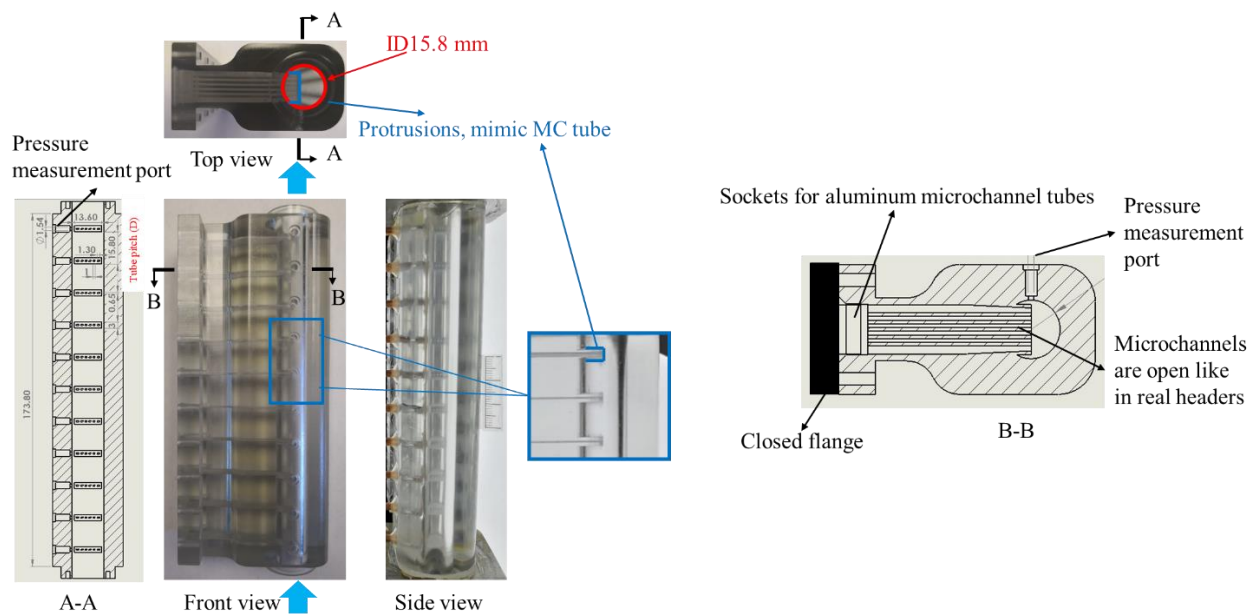


**Figure 10:** Visualization and pressure drop measurement part

The total length of this part is 173.8 mm. Both ends of the section are connected to a steel structure then two valves, the same as the sensor part. A high-speed camera will be used to capture flow regimes with a resolution of 512x512 and a speed of 2200 frames per second (fps). Pressure measurement ports are named 1 to 10 from low to high (Figure 11). To measure the pressure difference, port number 10 (assumed to be the lowest pressure port) is chosen to be the pressure baseline (connected to the lower-pressure input of the DP sensor). All other nine ports are connected to the higher-pressure input of the DP sensor by switching in a ball-valve system. The total pressure drop (including hydrostatic, frictional, local, and expansion pressure drop) between two ports (such as 1-2, 2-3, etc.) can be measured and calculated. By this method, the instrumental uncertainties from using multiple DP sensors can be reduced. All clear PFA tubes connecting the DP sensor and the tested ports are heated, and no liquid slugs that may affect pressure drop measurements are observed in the tubes.

Both the sensor part and the visualization/pressure drop part are installed at the same height in the facility. They have the same inlet structures, such as tubes and valves. By controlling the valves, refrigerant can pass through either part. Hence, it is assumed the results of void fraction, pressure drop, and flow regime are the same at both parts for the same inlet condition. Detailed calibration procedures of the sensors to measure void fraction in headers based on visualization, pressure drop, and capacitive signals are reported in the following paper.

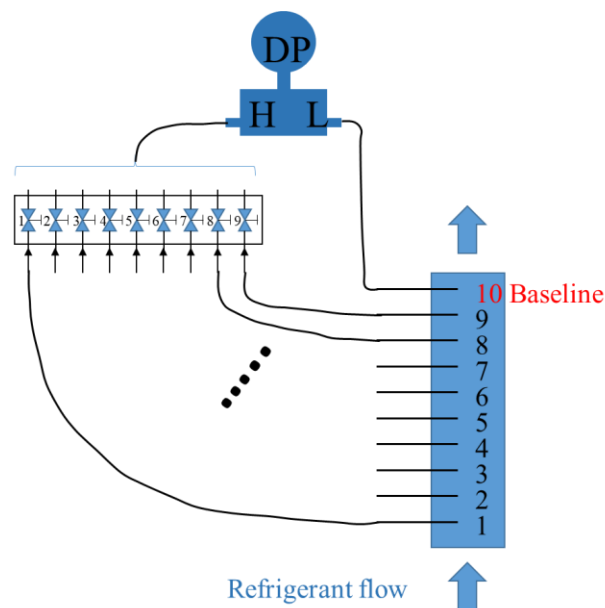


**Figure 11:** Schematic of the pressure measurement rig

### 3.3 Preliminary validation

The previous study indicates capacitive sensors with two-concave-plate configuration are capable of measuring void fraction and characterizing flow regimes of two-phase flow. However, the electric field within the sensor is not uniform. It is necessary to calibrate the sensor before further measurements can be applied (reported in the next paper). Preliminary validations are also needed before calibration to test whether all 11 sensors can provide reasonable signals regarding different void fractions.

The sensor part is put in the horizontal configuration for the validation procedure. Capacitive signals for two base points are first measured (Figure 12a): capacitive signals for full vapor phase ( $C_{Vapor}$ ) and full liquid phase ( $C_{Liquid}$ ).  $C_{Liquid}$  is obtained at 14.5 °C. Some researchers (dos Reis & Goldstein, 2005; Olivier et al., 2015) indicated that the effect of temperature on relative permittivity of refrigerant vapor phase could be neglected. Hence,  $C_{Vapor}$  is measured at room temperature. After signals of the two base points are determined, the refrigerant is filled into the part with different liquid levels, and both valves A and B are closed. The capacitive signals from all 11 sensors for each liquid level ( $C_{measured}$ ) are measured (Figure 12b).



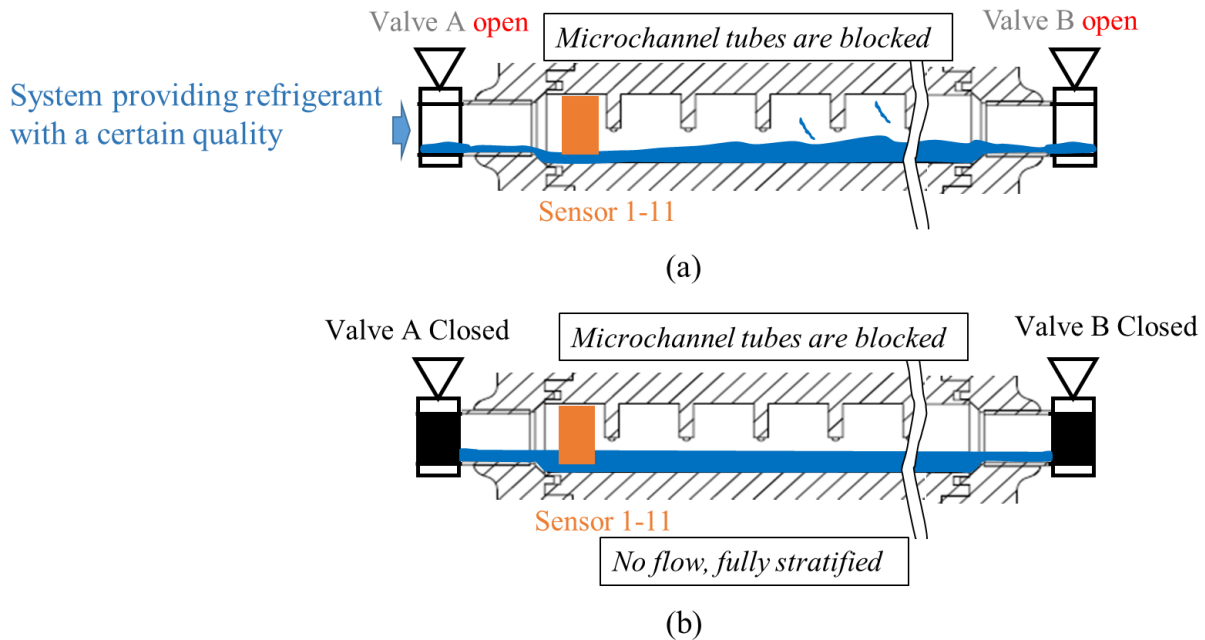


**Figure 12:** Schematic of the pressure measurement rig

Time-averaged  $C_{Vapor}$ ,  $C_{Liquid}$  and  $C_{measured}$  are also calculated:  $\overline{C_{Vapor}}$ ,  $\overline{C_{Liquid}}$  and  $\overline{C_{measured}}$ . Time-averaged normalized capacitance  $\overline{C_{norm}}$  are defined as follows:

$$\overline{C_{norm}} = \frac{\overline{C_{measured}} - \overline{C_{Vapor}}}{\overline{C_{Liquid}} - \overline{C_{Vapor}}} \quad (1)$$

The denominator shows the entire range of signal difference (from full vapor to full liquid). It is assumed constant for the duration of the one set of experiments. The numerator shows how much larger the measured signal is than the full vapor condition. Hence, the normalized signals are typically from 0 (fully vapor) to 1 (fully liquid). If all 11 sensors can provide similar results regarding a specific refrigerant liquid level, the sensors are validated preliminarily, and further calibration will be proposed in the future study.

Figure 13 shows the signals from 11 sensors regarding different liquid levels, including full vapor and liquid conditions. As the liquid level becomes higher, normalized signals from all sensors are larger. This agrees with the expected results. However, for a specific liquid level, normalized signals from 11 sensors do not equal. This means the sensors are not identical due to the nature of hand-made. If the sensor building procedure becomes standardized in future studies, the sensor performance will be better. Furthermore, the preliminary results also indicate the necessity of the calibration. It is important to find the relation between local void fractions and capacitive signals for each sensor. The calibration procedure will be discussed in the following paper.

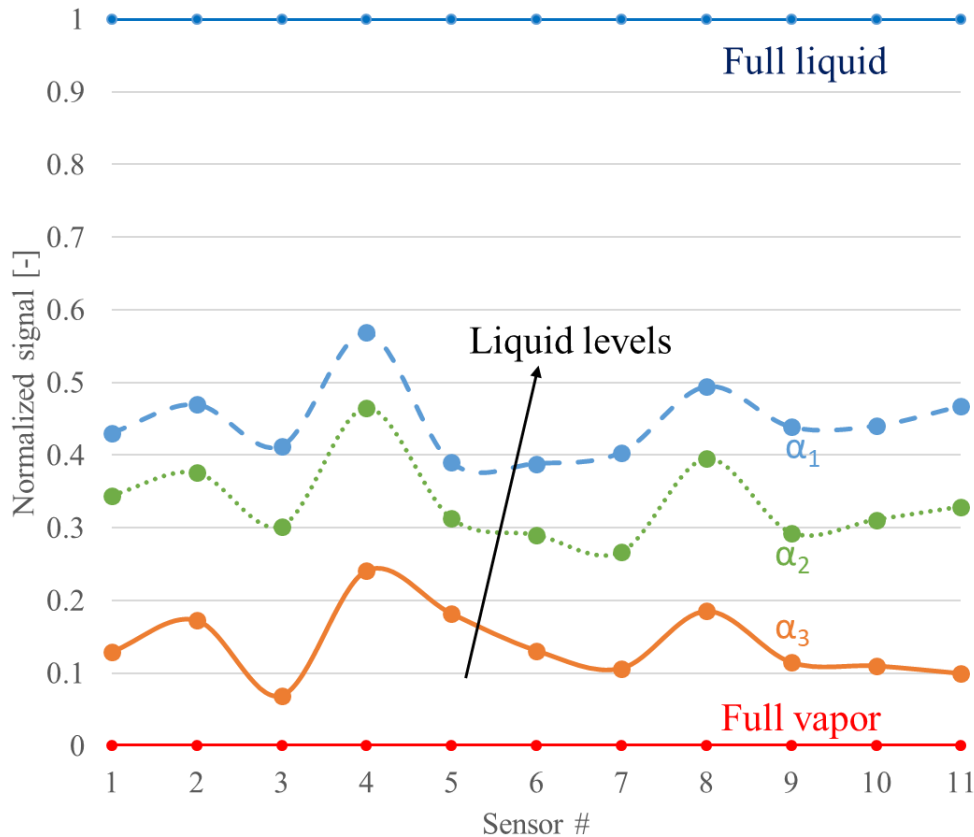


**Figure 13:** Normalized signals from 11 sensors regarding different liquid levels

#### 4. CONCLUSIONS

This paper presents the design of capacitive sensors for measuring void fractions in headers of microchannel heat exchangers with R134a. The sensors utilize the differences of permittivity (dielectric constant) between the liquid and vapor phases of R134a. The total length of the tested header is 185.8 mm, with an inner diameter of 15.8 mm (D). The header is assembled from eleven 3D printed partitions. Each partition has one individual sensor, protrusion, and socket for the microchannel tube connection. Each sensor has two concave-plate electrodes with the axial length of the half inner diameter ( $D/2$ ). Hence, eleven capacitive sensors, which are located between protrusions, measure the void fraction simultaneously. Visualization and pressure drop results along the headers are also necessary to study the void fraction in headers. A separate tested header with identical inner geometry is built. It is fully transparent and has ten pressure measurement ports. Preliminary validation of the sensors is also presented in this paper. Signals from all eleven sensors increase as the refrigerant liquid level becomes higher. However, signals from sensors are not the same. This is because all sensors are not identical due to the nature of hand-made. Further calibrations are needed before sensors are used to measure void fractions in headers.

#### NOMENCLATURE

C	Capacitance signals	(pF)
D	Inner diameter	(mm)
DP	Differential pressure	(kPa)
L	Axial electrode length	(mm)
P	Absolute pressure	(kPa)
R	Shield inner diameter	(mm)
t	Dielectric layer thickness	(mm)

$\alpha$	Void fraction	(-)
$\beta$	electrode angle	(°)

**Subscript**

Vapor	Vapor phase
Liquid	Liquid phase
measured	Measured values
norm	Normalized

**REFERENCES**

- Abouelwafa, M. S. A., & Kendall, E. J. M. (1980). The use of capacitance sensors for phase percentage determination in multiphase pipelines. *IEEE Transactions on Instrumentation and measurement*, 29(1), 24-27.
- Canière, H. (2010). Flow Pattern Mapping of Horizontal Evaporating Refrigerant Flow Based on Capacitive Void Fraction Measurements (Ph. D. thesis) Ghent University. *Ghent University*.
- Canière, H., T'Joel, C., Willockx, A., De Paepe, M., Christians, M., Van Rooyen, E., . . . Meyer, J. (2007). Horizontal two-phase flow characterization for small diameter tubes with a capacitance sensor. *Measurement Science and Technology*, 18(9), 2898.
- Canière, H., T'Joel, C., Willockx, A., & De Paepe, M. (2008). Capacitance signal analysis of horizontal two-phase flow in a small diameter tube. *Experimental Thermal and Fluid Science*, 32(3), 892-904.
- De Kerpel, K. (2015). *Refrigerant two-phase flow behaviour and pressure drop up-and downstream of a sharp return bend*. Ghent University,
- dos Reis, E., & Goldstein, L. (2005). A procedure for correcting for the effect of fluid flow temperature variation on the response of capacitive void fraction meters. *Flow Measurement and Instrumentation*, 16(4), 267-274.
- Hrnjak, P., & Litch, A. D. (2008). Microchannel heat exchangers for charge minimization in air-cooled ammonia condensers and chillers. *International journal of refrigeration*, 31(4), 658-668. doi:<https://doi.org/10.1016/j.ijrefrig.2007.12.012>
- Jaworek, A., & Krupa, A. (2004). Gas/liquid ratio measurements by rf resonance capacitance sensor. *Sensors and Actuators A: Physical*, 113(2), 133-139.
- Jaworek, A., & Krupa, A. (2010). Phase-shift detection for capacitance sensor measuring void fraction in two-phase flow. *Sensors and Actuators A: Physical*, 160(1), 78-86.
- Olivier, S., Meyer, J., Elton, L., Müller, C., Martin, S. J., Huisseune, H., . . . Marzo, S. (2015). Measured void fraction and heat transfer coefficients during condensation. *Sort*, 100, 250.
- Qian, H., & Hrnjak, P. (2019). Void Fraction Measurement and Flow Regimes Visualization of R134a in Horizontal and Vertical ID 7 mm Circular Tubes. *International journal of refrigeration*. doi:<https://doi.org/10.1016/j.ijrefrig.2019.04.018>
- Qian, H., & Hrnjak, P. (2020). Mass measurement based calibration of a capacitive sensor to measure void fraction for R134a in smooth tubes. *International journal of refrigeration*, 110, 168-177. doi:<https://doi.org/10.1016/j.ijrefrig.2019.10.019>
- Qian, H., & Hrnjak, P. (2021). Characterization of R134a two-phase flow regimes in horizontal and vertical smooth tubes with capacitive sensors. *International journal of refrigeration*. doi:<https://doi.org/10.1016/j.ijrefrig.2021.01.015>

**ACKNOWLEDGEMENT**

This study is supported by the Air-Conditioning and Refrigeration Center (ACRC) at the University of Illinois at Urbana-Champaign (UIUC). Authors would like to acknowledge the technical support from Creative Thermal Solutions Inc. (CTS).